

The Longitudinal Photon, Transverse Nucleon, Single-Spin Asymmetry in Exclusive Pion Electroproduction

D. Gaskell,¹ G.M. Huber,² and G. Warren¹

¹*Jefferson Lab, Newport News, VA 23606 USA*

²*University of Regina, Regina, SK S4S-0A2 Canada*

Abstract

We intend to measure the target single-spin asymmetry in the exclusive pion production reaction $\vec{p}(e, e'\pi^+)n$ reaction, using a transversely polarized ^1H target. This polarization variable has been noted as being especially sensitive to the spin-flip generalized parton distribution (GPD) \tilde{E} , and factorization studies have indicated that precocious scaling is likely to set in at moderate $Q^2 \sim 2-4$ $(\text{GeV}/c)^2$, as opposed to the absolute cross section, where scaling is not expected until $Q^2 \geq 10$ $(\text{GeV}/c)^2$. Furthermore, this variable has been noted as being important for the reliable extraction of the charged pion form factor from pion electroproduction. We intend to pursue this study using the proposed BETA electromagnetic calorimeter in coincidence with the HMS spectrometer, and with the UVa polarized NH_3 target. The calorimeter has significant vertical acceptance, and so allows data to be obtained over a large range of t at $Q^2 \sim 2$ $(\text{GeV}/c)^2$, $W \sim 2$ GeV and $x \sim 0.4$, and with favorable polarization angle relative to the virtual photon momentum. **A crucial aspect of our experiment is the Rosenbluth L/T separation.** Unlike other ongoing or proposed experiments, where the dominance of the longitudinal contribution to the spin asymmetry at these Q^2 is simply assumed, we intend to demonstrate whether this is in fact the case. This is important, because factorization has only been proven for the case of longitudinal photons. Data from this experiment will thus indicate whether the precocious scaling expectations of the GPD formalism will be ultimately realized, as well as helping to constrain longitudinal backgrounds possibly complicating the extraction of the pion form factor from electroproduction experiment data.

I. SCIENTIFIC JUSTIFICATION

A. Generalized Parton Distributions and Contribution from the Pion Pole

In recent years, much progress has been made in the theory of generalized parton distributions (GPDs). Unifying the concepts of parton distributions and of hadronic form factors, they contain a wealth of information about how quarks and gluons make up hadrons. The key difference between the usual parton distributions and their generalized counterparts can be seen by representing them in terms of the quark and gluon wavefunctions of the hadron. While the usual parton distributions are obtained from the squared hadron wavefunction representing the probability to find a parton with specified polarization and longitudinal momentum fraction x in the fast moving hadron (Fig. 1a), GPDs represent the interference of different wavefunctions, one where the parton has momentum fraction $x + \xi$ and one where this fraction is $x - \xi$ (Fig. 1b). GPDs thus correlate different parton configurations in the hadron at the quantum mechanical level. A special kinematic regime is probed in deep exclusive meson production, where the initial hadron emits a quark-antiquark or gluon pair (Fig. 1c). This has no counterpart in the usual parton distributions and carries information about $q\bar{q}$ and gg -components in the hadron wavefunction.

Apart from the momentum fraction variables x and ξ , GPDs depend on the four momentum transfer t . This is an independent variable, because the momenta p and p' may differ in either their longitudinal or transverse components. GPDs thus interrelate the longitudinal and transverse momentum structure of partons within a fast moving hadron.

In order to access the physics contained within GPDs, one is restricted to the hard scattering regime. An important feature of hard scattering reactions is the possibility to separate clearly the perturbative and nonperturbative stages of the interaction. Qualitatively speaking, the presence of a hard probe allows one to create small size quark-antiquark and gluon configurations, whose interactions are described by perturbative QCD (pQCD). The non-perturbative stage of the reaction describes how the hadron reacts to this configuration, or how this probe is transformed into hadrons. This separation is the so-called factorization property of hard reactions. Hard exclusive meson electroproduction was first shown to be factorizable in Ref. [2]. This factorization applies when the virtual photon is longitudinally polarized, which corresponds to a small size configuration compared to a transversely

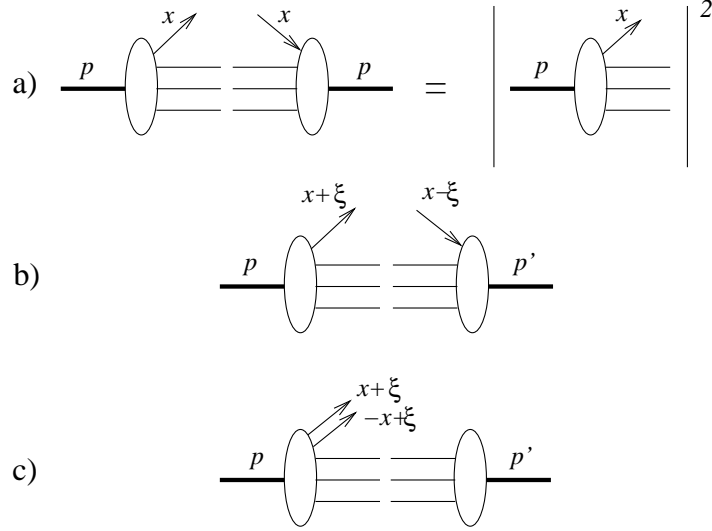


FIG. 1: (a) Usual parton distribution, representing the probability to find a parton with momentum fraction x in the nucleon. (b) GPD in the region where it represents the emission of a parton with momentum fraction $x + \xi$ and its reabsorption with momentum fraction $x - \xi$. (c) GPD in the region where it represents the emission of a quark-antiquark pair, and has no counterpart in the usual parton distributions. This figure has been adapted from Ref. [1].

polarized photon.

GPDs are universal quantities and reflect the structure of the nucleon independently of the reaction which probes the nucleon. At leading twist-2 level, the nucleon structure information can be parameterized in terms of four quark chirality conserving GPDs, denoted H , E , \tilde{H} and \tilde{E} . H and E are summed over quark helicity, while \tilde{H} and \tilde{E} involve the difference between left and right handed quarks. H and \tilde{H} conserve the helicity of the proton, while E and \tilde{E} allow for the possibility that the proton helicity is flipped. Because quark helicity is conserved in the hard scattering regime, the produced meson acts as a helicity filter. In particular, leading order QCD predicts that vector meson production is sensitive only to the unpolarized GPDs, H and E , whereas pseudoscalar meson production is sensitive only to the polarized GPDs, \tilde{H} and \tilde{E} . In contrast, deeply virtual compton scattering (DVCS) depends at the same time on both the polarized (\tilde{H} and \tilde{E}) and the unpolarized (H and E) GPDs. This makes hard meson electroproduction reactions complementary to the DVCS process, as it provides an additional tool to disentangle the different GPDs [3].

Besides coinciding with the parton distributions at vanishing momentum transfer ξ , the

GPDs have interesting links with other nucleon structure quantities. Their first moments are related to the elastic form factors of the nucleon through model-independent sum rules [4]:

$$\sum_q e_q \int_{-1}^{+1} dx H^q(x, \xi, t) = F_1(t), \quad (1)$$

$$\sum_q e_q \int_{-1}^{+1} dx E^q(x, \xi, t) = F_2(t), \quad (2)$$

$$\sum_q e_q \int_{-1}^{+1} dx \tilde{H}^q(x, \xi, t) = G_A(t), \quad (3)$$

$$\sum_q e_q \int_{-1}^{+1} dx \tilde{E}^q(x, \xi, t) = G_P(t), \quad (4)$$

where e_q is the charge of the relevant quark, $F_1(t)$, $F_2(t)$ are the Dirac and Pauli elastic nucleon form factors, and $G_A(t)$, $G_P(t)$ are the isovector axial and pseudoscalar nucleon form factors. The t -dependence of $G_A(t)$ is poorly known, and although $G_P(t)$ is an important quantity, it remains highly uncertain because it is negligible at the momentum transfer of β -decay[5]. Because of PCAC, $G_P(t)$ alone receives contributions from $J^{PG} = 0^{--}$ states[6], which are the quantum numbers of the pion, and so \tilde{E} contains an important pion pole contribution (Fig. 2a).

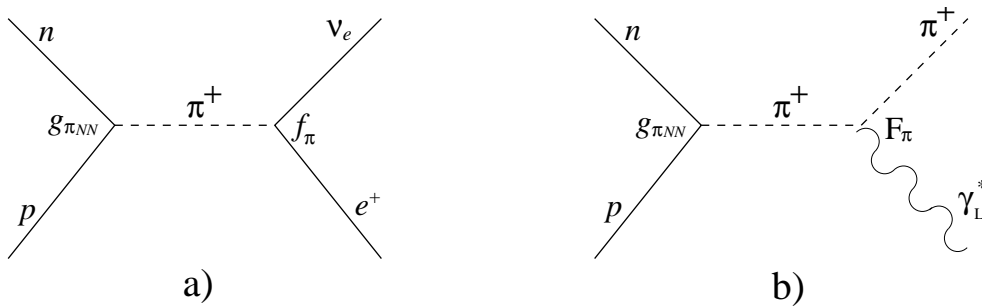


FIG. 2: (a) Pion pole contribution to $G_P(t)$, and hence to \tilde{E} . (b) Pion pole contribution to meson electroproduction at low $-t$.

Accordingly, Refs. [7, 8] have adopted the pion pole-dominated ansatz

$$\tilde{E}^{ud}(x, \xi, t) = F_\pi(t) \frac{\theta(\xi > |x|)}{2\xi} \phi_\pi\left(\frac{x + \xi}{2\xi}\right), \quad (5)$$

where $F_\pi(t)$ is the pion electromagnetic form factor, and ϕ_π is the pion distribution amplitude.

\tilde{E} cannot be related to already known parton distributions, and so experimental information about \tilde{E} via hard pion electroproduction can provide new information on nucleon structure which is unlikely to be available from any other source.

B. Single spin asymmetry in exclusive pion electroproduction

Frankfurt et al. [9] have considered a specific polarization observable which is the most sensitive observable to probe the spin-flip \tilde{E} . This variable is the single-spin asymmetry for exclusive π^+ production, $\vec{p}(e, e'\pi^+)n$, from a transversely polarized target, and is defined [8] as

$$A_{\perp} = \left(\int_0^{\pi} d\beta \frac{d\sigma_L^{\pi^+}}{d\beta} - \int_{\pi}^{2\pi} d\beta \frac{d\sigma_L^{\pi^+}}{d\beta} \right) \left(\int_0^{2\pi} d\beta \frac{d\sigma_L^{\pi^+}}{d\beta} \right)^{-1}, \quad (6)$$

where $d\sigma_L^{\pi^+}$ is the exclusive electroproduction cross section using longitudinally polarized photons and β is the angle between the target polarization vector and the reaction plane. Frankfurt et al. [9] have shown that this asymmetry must vanish if \tilde{E} is zero. If \tilde{E} is not zero, the asymmetry will display a $\sin\beta$ dependence. Their predicted asymmetry using the \tilde{E} ansatz from Ref. [11] is shown in Fig. 3.

Furthermore, it seems likely that a precocious factorization of the meson production amplitude into three parts – the overlap integral between the photon and pion wave functions, the hard interaction, and the GPD – will lead to a precocious scaling of A_{\perp} as a function of Q^2 at moderate $Q^2 \sim 2 - 4$ (GeV/c)² [9]. This precocious scaling arises from the fact that higher order corrections, which may be significant at low Q^2 , will likely cancel when one examines the ratio of two observables. The relatively low value of Q^2 is important, because it is accessible experimentally at Jefferson Lab and is relevant to the Jefferson Lab and HERMES programs. In contrast, the onset of scaling for the absolute cross section is only expected for much larger values of $Q^2 \geq 10$ (GeV/c)².

The recent HERMES single-spin asymmetry result in exclusive π^+ electroproduction was obtained for average values of $\langle x \rangle = 0.15$, $\langle Q^2 \rangle = 2.2$ (GeV/c)² and $\langle t \rangle = -0.46$ (GeV/c)² [12]. Using a hydrogen target polarized parallel to the incident electron beam, they observed an azimuthal polarization asymmetry and attributed this to the small target polarization component transverse to the reaction plane. This helped motivate their recent installation of a target with polarization transverse to the electron beam.

Jefferson Lab can make a unique contribution to studies of the π^+ transverse

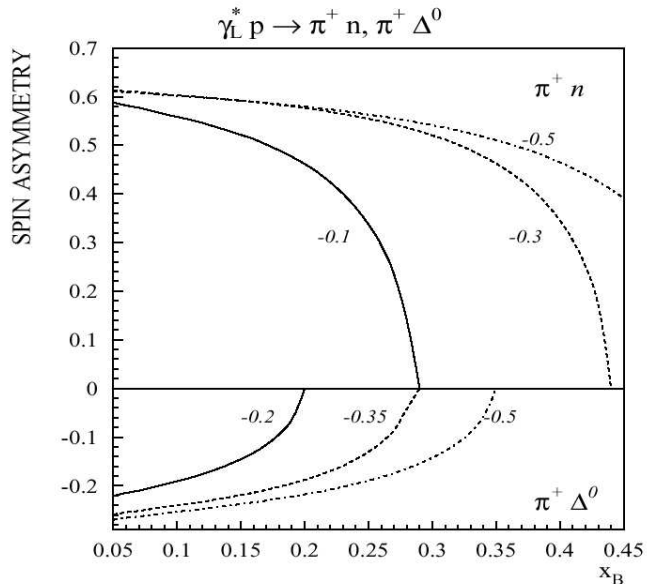


FIG. 3: Transverse single-spin asymmetry for the longitudinal electroproduction of $\pi^+ n$ and $\pi^+ \Delta^0$ at different values of t [indicated on the curves in $(\text{GeV}/c)^2$]. The asymmetry drops to zero at the parallel kinematic limit, which is different for each t value, because the definition of P_y is ill-defined at this point. This figure is taken from Ref. [10].

target asymmetry via the ability to take measurements at multiple beam energies and unambiguously isolate the longitudinal component of the asymmetry using a Rosenbluth separation. Unfortunately, due to the single beam energy, such a separation is not feasible at HERMES.

Refs. [3] and [10] also point out that the study of this single-spin asymmetry at low $-t$ is important for the reliable extraction of the pion form factor from electroproduction experiments (Fig. 2b). Investigations of hard exclusive π^+ electroproduction using a pQCD factorization model [13, 14] find that at $x = 0.3$ and $-t = -t_{min}$, the pion pole contributes about 80% of the longitudinal cross section. Since the single-spin asymmetry is an interference between pseudoscalar and pseudovector contributions, its measurement would help constrain the non-pole pseudovector contribution, and so assist the more reliable extraction of the pion form factor. The experimental study of the pion form factor has been identified as an important part of the JLab 12 GeV program [15], and the measurement of the single-spin asymmetry is a logical step in the support of that program.

C. Reasons why a Rosenbluth separation is required

Because transverse photon amplitudes are suppressed by $1/Q$, at very high Q^2 it is safe to assume that all observed meson production is due to longitudinal photons. At the $Q^2 \sim 2$ (GeV/c)² typical of the Jefferson Lab and HERMES programs, however, this is not the case. Bartl and Majerotto [16] have shown that the transverse single-spin asymmetry in exclusive π^+ electroproduction not only has contributions from the purely longitudinal amplitude discussed in Refs. [3, 8–10], but also has contributions from transverse-transverse and longitudinal-transverse interference amplitudes.

They express the transversely polarized target cross section as

$$\frac{d\sigma_{\perp}}{dt} = \frac{P_y p_{\pi} W}{KM} [Im Y_1 + \epsilon \cos 2\phi Im Y_2 + 2\epsilon Im Y_3 + \sqrt{2\epsilon(1+\epsilon)} \cos \phi Im Y_4], \quad (7)$$

where P_y is the target polarization component parallel to $\hat{q} \times \hat{p}_{\pi}$, p_{π} is the outgoing pion momentum in the virtual photon–nucleon center of mass, W is the invariant mass of the hadronic system, $K = (W^2 - M^2)/2M$ is the so-called equivalent photon energy, and

$$Y_1 = h_+^N h_+^{F*} + h_-^N h_-^{F*} \quad (8)$$

$$Y_2 = h_-^N h_-^{F*} - h_+^N h_+^{F*} \quad (9)$$

$$Y_3 = h_0^N h_0^{F*} \quad (10)$$

$$Y_4 = h_0^N h_-^{F*} - h_0^F h_-^{N*} \quad (11)$$

The h 's are helicity amplitudes, where the superscripts F and N indicate baryon spin-flip and non-spin-flip amplitudes, respectively, and the subscripts 0, +, – indicate virtual photon polarizations longitudinal, parallel to the scattering plane and perpendicular to the scattering plane. Thus, the desired term for study is Y_3 , but at HERMES and Jefferson Lab energies one can not ignore the contributions of Y_1 , Y_2 and Y_4 to the observed asymmetry. Y_1 is especially problematic, because it can only be separated from Y_3 with the use of a Rosenbluth separation. The transverse contributions to Y_1 can be estimated using a Regge model [17]. Preliminary indications are that the transverse photon transverse target asymmetry is smaller than the longitudinal photon transverse target asymmetry but nonzero, for JLab kinematics, and so the experiment must be designed from the beginning to account for this contribution.

Looking more thoroughly at the contributions to the transverse target asymmetry in the context of the (slightly modified) notation of Bartl and Majerotto [16], in the case of an

unpolarized beam and unpolarized target the virtual photoproduction cross section can be written as

$$\frac{d\sigma}{d\Omega} = \sigma_T + \epsilon \sigma_L + \epsilon \sigma_{TT} \cos 2\phi + \sqrt{\frac{1}{2}\epsilon(1+\epsilon)} \sigma_{LT} \cos \phi, \quad (12)$$

where σ_T , σ_L , σ_{TT} , and σ_{LT} are the usual (modulo some factors of 2) transverse, longitudinal and interference cross sections and ϕ is the azimuthal angle between the reaction plane and the scattering plane. These cross sections can be broken down into helicity amplitudes as follows:

$$\sigma_T = \frac{p_\pi W}{KM} \frac{1}{2} (|h_+^N|^2 + |h_+^F|^2 + |h_-^N|^2 + |h_-^F|^2) \quad (13)$$

$$\sigma_L = \frac{p_\pi W}{KM} (|h_0^N|^2 + |h_0^F|^2) \quad (14)$$

$$\sigma_{TT} = \frac{p_\pi W}{KM} \frac{1}{2} (|h_-^N|^2 + |h_-^F|^2 - |h_+^N|^2 - |h_+^F|^2) \quad (15)$$

$$\sigma_{LT} = \frac{p_\pi W}{KM} 2\text{Re}(h_0^N h_-^{N*} + h_0^F h_-^{F*}). \quad (16)$$

For a polarized target, there is an additional contribution to the cross section:

$$\begin{aligned} \sigma_t = P_x & \left[-\sqrt{2\epsilon(1+\epsilon)} \sin \phi \sigma_{LT}^x - \epsilon \sin 2\phi \sigma_{TT}^x \right] \\ & - P_y \left[\sigma_{TT}^y + \epsilon \cos 2\phi \sigma_{TT'}^y + 2\epsilon \sigma_L^y + \sqrt{2\epsilon(1+\epsilon)} \cos \phi \sigma_{LT}^y \right] \\ & + P_z \left[\epsilon \sin 2\phi \sigma_{TT}^z + \sqrt{2\epsilon(1+\epsilon)} \sin \phi \sigma_{LT}^z \right], \quad (17) \end{aligned}$$

where the various cross sections are given by:

$$\sigma_{LT}^x = \frac{p_\pi W}{KM} \text{Im} X_1 \quad (18)$$

$$\sigma_{TT}^x = \frac{p_\pi W}{KM} \text{Im} X_2 \quad (19)$$

$$\sigma_{TT}^y = \frac{p_\pi W}{KM} \text{Im} Y_1 \quad (20)$$

$$\sigma_{TT'}^y = \frac{p_\pi W}{KM} \text{Im} Y_2 \quad (21)$$

$$\sigma_L^y = \frac{p_\pi W}{KM} \text{Im} Y_3 \quad (22)$$

$$\sigma_{LT}^y = \frac{p_\pi W}{KM} \text{Im} Y_4 \quad (23)$$

$$\sigma_{TT}^z = \frac{p_\pi W}{KM} \text{Im} Z_2 \quad (24)$$

$$\sigma_{LT}^z = \frac{p_\pi W}{KM} \text{Im} Z_1. \quad (25)$$

The Y amplitudes have been defined earlier, and the X and Z amplitudes are made up of additional linear combinations of helicity amplitudes. The subscripts on each ‘‘cross section’’ denote whether they contain longitudinal amplitudes, transverse amplitudes, or both.

The x , y , and z components of the target polarization are denoted P_x , P_y , and P_z . In the co-ordinate system used here, the z direction is along the virtual photon direction (\vec{q}), the y -axis is perpendicular to the hadron reaction plane (in the direction of $\vec{q} \times \vec{p}_\pi$), and the x direction is given by $\hat{y} \times \hat{z}$.

In this discussion, we are interested in the transverse target asymmetries, so we will ignore the terms proportional to P_z . If we define β to be the azimuthal angle between the component of the target polarization perpendicular to \vec{q} (P_\perp) and the hadron reaction plane, we can re-express P_x and P_y as:

$$P_x = P_\perp \cos \beta \tag{26}$$

$$P_y = P_\perp \sin \beta \tag{27}$$

Note that if we set all the transverse amplitudes to zero in the above expressions for the unpolarized + polarized cross sections, we are left with

$$\frac{d\sigma}{d\Omega} = \epsilon \sigma_L - 2\epsilon \sigma_L^y P_\perp \sin \beta . \tag{28}$$

This is the basis for the exclusive pion transverse target asymmetry defined in Ref.[8], which essentially extracts the ratio of σ_L^y to σ_L . For very large values of Q^2 , transverse amplitudes should be small, so the above asymmetry can likely be extracted with no explicit L-T separation to isolate the longitudinal components. However, at the kinematics accessible at JLab one can not assume that this will be the case, so we must take care to address the transverse contributions appropriately.

Experimentally, the angle between the target polarization and the reaction plane, β , and the angle between the scattering and reaction planes, ϕ , are not independent. If the target polarization is at some angle, Φ , relative to the scattering plane, then $\beta = \Phi - \phi$. For the experimental set-up that will be discussed here, Φ is relatively constant, so it will be useful to re-express the above cross sections in terms of β and Φ . The polarized target cross section

then becomes:

$$\begin{aligned}
\sigma_t = & -P_\perp \sin \beta [\sigma_{TT}^y + 2\epsilon \sigma_L^y] \\
& - P_\perp \sin \beta [\epsilon(\cos 2\Phi \cos 2\beta + \sin 2\Phi \sin 2\beta) \sigma_{TT'}^y] \\
& - P_\perp \sin \beta \left[\sqrt{2\epsilon(1+\epsilon)}(\cos \Phi \cos \beta + \sin \Phi \sin \beta) \sigma_{LT}^y \right] \\
& - P_\perp \cos \beta \left[\sqrt{2\epsilon(1+\epsilon)}(\sin \Phi \sin \beta - \cos \Phi \cos \beta) \sigma_{LT}^x \right] \\
& - P_\perp \cos \beta [\epsilon(\sin 2\Phi \sin 2\beta - \cos 2\Phi \cos 2\beta) \sigma_{TT}^x]. \quad (29)
\end{aligned}$$

By using a target with protons polarized perpendicular to \vec{q} , but roughly in the scattering plane $\Phi = 0$, the above expression simplifies to (setting all the $\sin \Phi$ terms to zero)

$$\begin{aligned}
\sigma_t = & -P_\perp \sin \beta [\sigma_{TT}^y + 2\epsilon \sigma_L^y] \\
& - P_\perp \sin \beta [\epsilon(\cos 2\Phi \cos 2\beta) \sigma_{TT'}^y] \\
& - P_\perp \sin \beta \left[\sqrt{2\epsilon(1+\epsilon)}(\cos \Phi \cos \beta) \sigma_{LT}^y \right] \\
& + P_\perp \cos \beta \left[\sqrt{2\epsilon(1+\epsilon)}(\cos \Phi \cos \beta) \sigma_{LT}^x \right] \\
& + P_\perp \cos \beta [\epsilon(\cos 2\Phi \cos 2\beta) \sigma_{TT}^x]. \quad (30)
\end{aligned}$$

From the above equation, it is clear that to extract the (longitudinal photon) transverse target asymmetry it is necessary to first isolate the $\sin \beta$ Fourier component of the polarized target cross section[21]. Once that has been accomplished, one must then separate the σ_L^y term from the σ_{TT}^y term via a Rosenbluth-type separation. This is what we propose to do in this experiment.

II. EXPERIMENTAL METHOD

A. Set-up and Kinematics

We intend to pursue this measurement in Hall C, using the HMS in coincidence with the proposed BETA electromagnetic calorimeter. The calorimeter would be used to detect the scattered electron, while the π^+ will be detected in the HMS. The UVa polarized NH_3 would be utilized, with the polarization vector oriented in the horizontal plane, nearly transverse to the q -vector. This configuration has a number of important advantages.

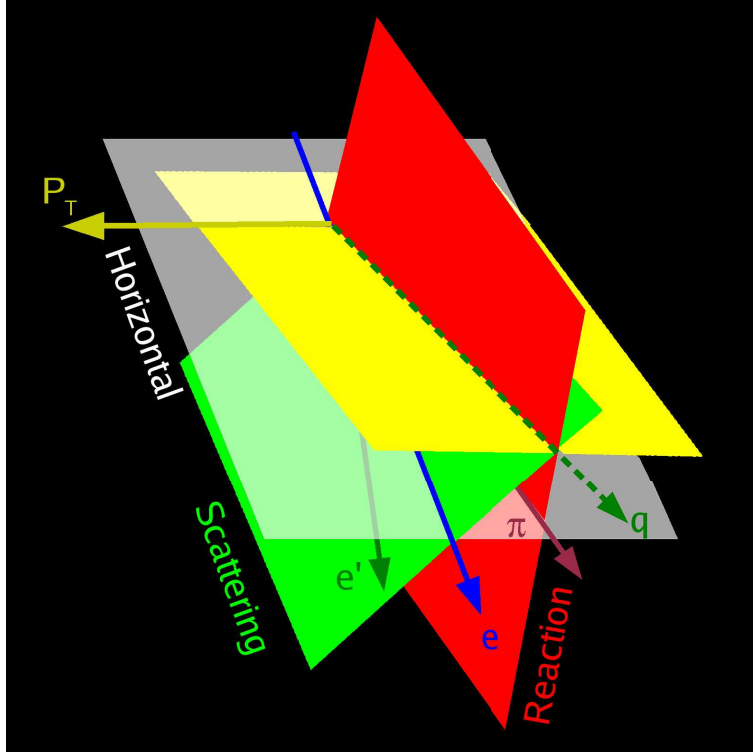


FIG. 4: Schematic diagram of the experiment. The incident electron beam and the target polarization P_t are located in the horizontal plane. Here, the scattered electron e' is detected below the horizontal plane, which forces q to be above the plane. The π^+ is detected in the HMS, nearly in the horizontal plane, in this case directly below q . This forces the reaction plane to be nearly vertical, regardless of where in the calorimeter the electron was detected. P_t is nearly orthogonal to q , as desired.

The measurement of the transverse single-spin asymmetry requires the detection of the π^+ in non-parallel kinematics. It is the component of the target polarization parallel to $\hat{q} \times \hat{p}_\pi$ that is important (Eqn. 7), and this direction is uniquely defined only in non-parallel kinematics. This is accomplished by the use of the electromagnetic calorimeter, with significant vertical acceptance, and is shown schematically in Fig. 4. The scattered electron is detected at some vertical position on the calorimeter. This forces the scattering plane and the q -vector to be non-horizontal. The π^+ is detected in the HMS, either above or below \vec{q} , depending on whether the scattered electron was detected at above or below the horizontal plane. The target polarization vector is located in the horizontal plane, parallel to $\hat{q} \times \hat{p}_\pi$, and remains nearly transverse to \vec{q} , regardless of the value of ϕ (the angle between the

scattering and reaction planes). The vertical calorimeter thus allows the use of an already existing target to perform the measurement, with an efficient use of the requested beam time.

Simple $\vec{p}(e, e' \pi^+)n$ kinematics for $Q^2 = 2.0$ (GeV/c) 2 , $W = 2.0$ GeV							
$E_{e'}$	$\theta_{e'}$	θ_π	$\Theta_{\pi q}$	p_π	$-t$	x	z
(GeV)	(deg)	(deg)	(deg)	(GeV)	(GeV/c) 2		
High $\epsilon = 0.59$ setting, $E_e = 4.40$ GeV							
1.672	30.22	-15.90	0.0	2.619	0.195	0.391	0.962
1.672	30.22	-15.90	± 5.0	2.568	0.231	0.391	0.943
1.672	30.22	-15.90	± 10.0	2.428	0.328	0.391	0.891
1.672	30.22	-15.90	± 15.0	2.222	0.472	0.391	0.816
1.672	30.22	-15.90	± 20.0	1.989	0.636	0.391	0.731
Low $\epsilon = 0.32$ setting, $E_e = 3.50$ GeV							
0.772	50.94	-11.25	0.0	2.619	0.195	0.391	0.962
0.772	50.94	-11.25	± 5.0	2.568	0.231	0.391	0.943
0.772	50.94	-11.25	± 10.0	2.428	0.328	0.391	0.891
0.772	50.94	-11.25	± 15.0	2.222	0.472	0.391	0.816
0.772	50.94	-11.25	± 20.0	1.989	0.636	0.391	0.731

TABLE I: Kinematic settings for the experiment, uncorrected for deflection in the polarized target magnetic field, to give a quick sense of the experiment set-up. Actual kinematic coverage, with the deflection in the target magnetic field included, is given by the MC simulation studies discussed in the Sec. IIB. $\Theta_{\pi q}$ is the vertical lab angle of the π^+ with respect to \vec{q} , due to the scattered electron acceptance in the calorimeter. Each vertical scan, corresponding to a $-t$ distribution at fixed x , would be taken in a single setting, with the HMS set for a central momentum of 2.350 GeV/c.

BETA (Big Electron Telescope Array) is based on the electromagnetic calorimeter currently being assembled for the G_E^p/G_M^p experiment in Hall C, E01-109, but with the addition of gas Cerenkov and lucite Cerenkov detectors for clean electron identification with a π^\pm rejection of at least 1000:1. The full technical specifications of BETA are given in the Spin Asymmetries on the Nucleon Experiment (SANE) proposal before this PAC. We would use

BETA without modification, at the central kinematic settings listed in Table I.

The University of Virginia polarized NH_3 target uses microwave pumping, low temperature (1 K) and high magnetic field (5 T) to achieve proton polarizations up to 95%, via the principle of dynamic nuclear polarization. During the experiment, the target material is exposed to 140 GHz microwaves to drive the hyperfine transition, which aligns the nucleon spins. The target polarization is reduced by a few percent by beam-induced heating, and then continues to decrease slowly due to beam-induced radiation damage. Most of the radiation damage is repaired by annealing the target at about 80 K, until the accumulated dose reaches $\sim 2 \times 10^{17}$ electrons, at which point the target material needs to be changed. There are two target cells, so an anneal is performed approximately once per day.

The target cell is 3 cm in length, and the magnetic field coils have a 50° conical shaped aperture (the bore) along the magnetic field axis, and a 34° wedge shaped aperture (the split) along the vertically oriented midplane. For this experiment, the target would be oriented with the magnetic field at an angle of 78° with respect to the incident electron beam. This results in the target polarization being aligned transverse to the q -vector. The unscattered electron beam, as well as the HMS, would view through the split of the coil, and the calorimeter would view through the bore.

As part of the program to minimize the sources of systematic errors, the target polarization will be reversed after each anneal by adjusting the microwave frequency. We would also prefer to reverse the magnetic field direction after every other anneal, although this may pose technical problems with the polarized target chicane and dumping the unscattered electrons.

B. Simulation of the Experiment - Acceptance

Preliminary simulations of this proposed measurement have been carried out using the standard Hall C Monte Carlo, SIMC. In this case, we have used a modified version of SIMC, which includes the effects of the 5 T polarized target field on both the forward-going particles and on the reconstruction. SIMC is primarily an aperture-checking, magnetic optics based Monte Carlo and does not generally include simulations of detector response. Therefore, the calorimeter has been simulated by transporting electrons to the face of the calorimeter and smearing the position and energy of the particle by the nominal calorimeter resolution

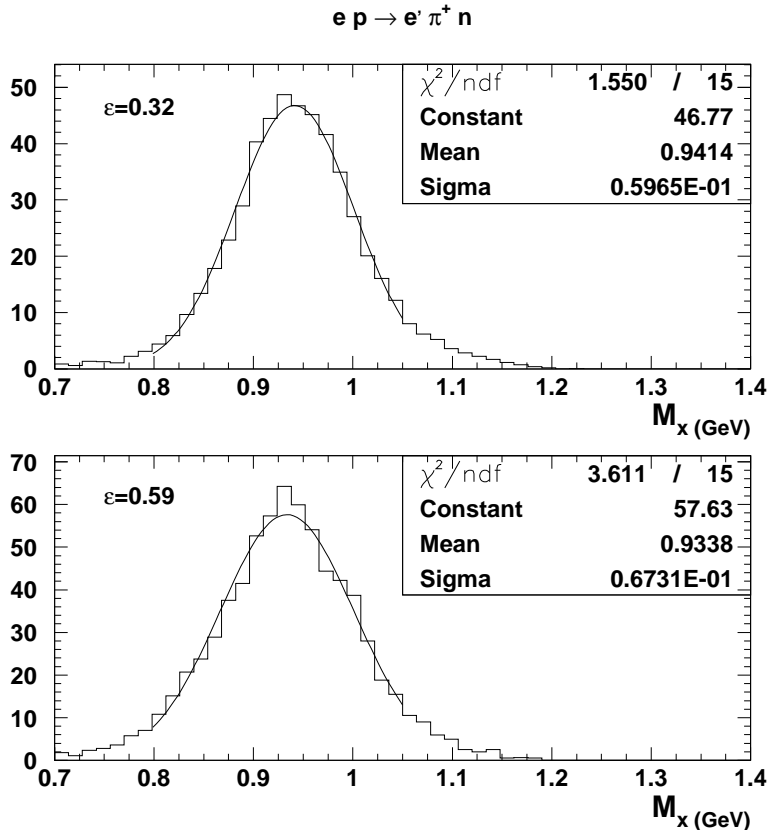


FIG. 5: Simulated missing mass distributions for $[(e, e'\pi^+)n]$: electrons are detected in the proposed BETA detector and pions are detected in the HMS. A Gaussian fit to the missing mass peak gives a resolution of $\sigma \approx 60$ (67) MeV at low (high) epsilon.

($5\%/\sqrt{E}$ in energy and 4 mm in position).

One of the first considerations in this experiment is the ability to distinguish the exclusive final state. With magnetic spectrometers, this is typically not a problem in the $(e, e'\pi^+)$ reaction, but with the significantly worse energy resolution of a calorimeter, it must be investigated. Fig. 5 shows the simulated missing mass spectra for both of the ϵ settings listed in Table I. The missing mass resolution is quite good, and should be more than adequate for separating the exclusive final state from multiple pion production and the residual Δ final state. The contributions of 2π states should be further suppressed by the high values of z chosen for this experiment.

Ideally, one would like full coverage of the angle between the perpendicular target polarization and the reaction plane, β . In practice, this is difficult to achieve. However, as

discussed briefly in the previous section, the combination of the UVa polarized target and the acceptance of the proposed BETA detector maximizes our sensitivity to the $\sin\beta$ component of the cross section. This is shown in Fig. 6. The top panel shows the simulated β distribution assuming no target field. No $\sin\beta$ term was used to generate this distribution, hence the large number of simulated events in the vicinity of 90° and 270° is due to the acceptance of the experimental configuration. This type of β coverage is well-suited to extracting the $\sin\beta$ term of the polarized cross section given in Eqns. 29 and 30.

As seen in the bottom panel of Fig. 6, the target field significantly affects the observed β distribution. This is simply because the target field is mostly transverse to the scattered particle direction and biases the acceptance of the HMS (BETA) to favor particles that are initially moving in a downward (upward) trajectory. Note, however, that since the definition of β incorporates the direction of the target polarization, and since the target polarization can be reversed by adjustment of the pumping frequency without changing the magnetic field, one can regain the symmetry of the β acceptance (solid and dashed lines in the figure).

While the kinematics in Tab. I are for a particular Q^2 and W (or x_B), the large acceptance of BETA implies that we will sample a large range of x_B , Q^2 , and t . This is illustrated in Fig. 7 and Fig. 8.

C. Rates and Estimate of Uncertainties

The version of SIMC used for the above acceptance studies also includes radiative effects, pion decay, effects from multiple scattering, and pion electroproduction cross section models, so can be used to reliably extract rate estimates. In this case, the pion cross section used was a parameterization consistent with the separated cross sections extracted in the pion form-factor experiment, E93-021 [18].

The UVa polarized target is 3 cm long and made from $^{15}\text{NH}_3$ with a density of 0.917 g/cm^3 . However, rate estimates must account for the fact that the target material does not occupy all of the space along the 3 cm target cell length. This is the so-called packing fraction, and for $^{15}\text{NH}_3$ is typically ≈ 0.55 [19]. All rates are estimated assuming production from the hydrogen in the $^{15}\text{NH}_3$ target. With all of the above assumptions, and further implementing reasonable acceptance cuts and the phase-space matching cuts necessary for an L–T separation (see Fig. 7), we estimate approximately 233 (164) good pions per mC of

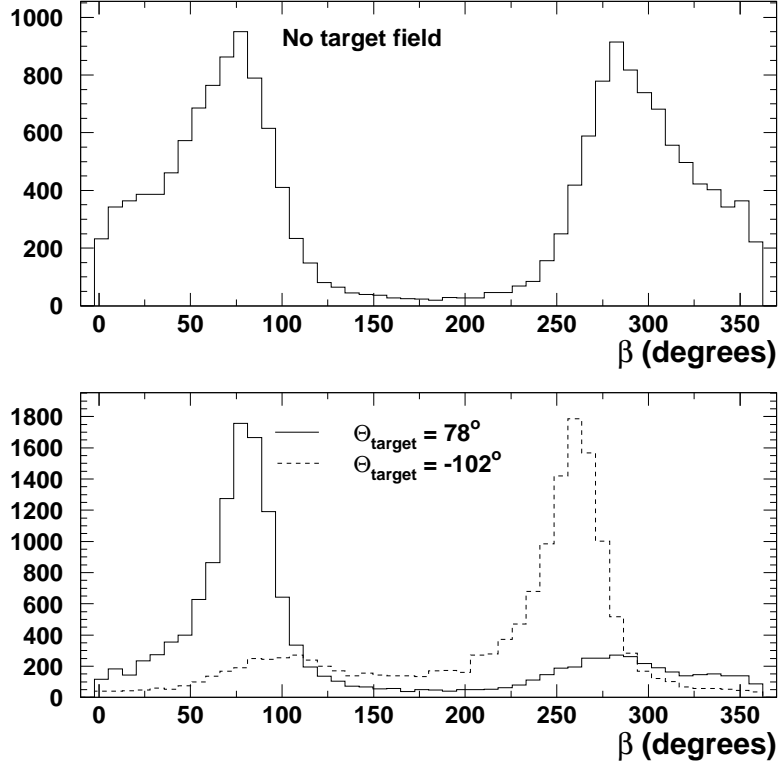


FIG. 6: Simulated distribution of azimuthal angle of the (transversely) polarized target with respect to the hadron reaction plane, β . The top plot shows the β distribution without the effects of the target field while the bottom plot shows the distribution including target field effects. Note that the acceptance is biased to $\beta = 90^\circ$ for the target polarization at 78° (beam left). Since the calculation of β incorporates the polarization vector of the target, however, we can recover the symmetry of the β acceptance by flipping the target polarization direction 180° .

charge on target at $\epsilon = 0.59$ ($\epsilon = 0.32$).

As seen in Fig. 8, the BETA acceptance allows us to sample a large phase space in t . If the data is broken into four t -bins, we can achieve statistics comparable to the estimated (uncorrelated) systematic uncertainty (see the later discussion) in each bin with $\approx 40,000$ events per ϵ setting. Assuming a beam current of 85 nA, this implies about 560 (796) hours of beam on target for $\epsilon = 0.59$ ($\epsilon = 0.32$).

The quantity we wish to extract is a ratio of two longitudinal cross sections. As typically defined (i.e., Eqn. 6), the transverse target asymmetry as written in our notation corresponds

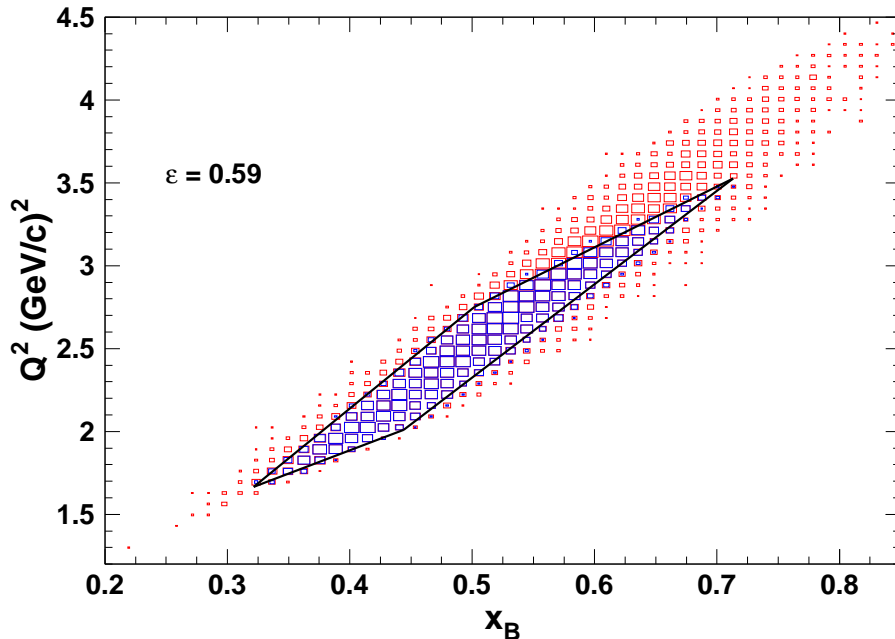


FIG. 7: Experimental acceptance in Q^2 and x_B for the $\epsilon = 0.59$ kinematic setting. The blue points enclosed in the “diamond” denote the region of overlap with the $\epsilon = 0.32$ setting.

to,

$$A_{\perp} = \frac{1}{P_{\perp}} \frac{2}{\pi} \frac{2\sigma_L^y}{\sigma_L}, \quad (31)$$

where σ_L^y and σ_L were defined earlier in Sec I-C. To obtain a rough estimate of the expected uncertainty in such a measurement, we assume the polarized target cross section has the following simplified form,

$$\sigma = \sigma_T + \epsilon\sigma_L - P_{\perp} \sin \beta (\sigma_T^y + \epsilon 2\sigma_L^y). \quad (32)$$

The final uncertainty in any L–T separated cross section is sensitive to the ratio of the longitudinal to transverse cross sections ($R = \frac{\sigma_L}{\sigma_T}$). The assumption of $1/Q$ suppression of transverse amplitudes implies that the transverse cross section should be about 2.4 times smaller than the longitudinal. On the other hand, Regge model calculations [17] indicate that for our kinematics $R = 1.4$ to 3.3. Finally, the Unitary Isobar MAID model [20] predicts that the L–T ratio is about 1.7. For the calculations here, we therefore assume an “average” of these three estimates of $R = 2$. The polarized longitudinal cross section is in general

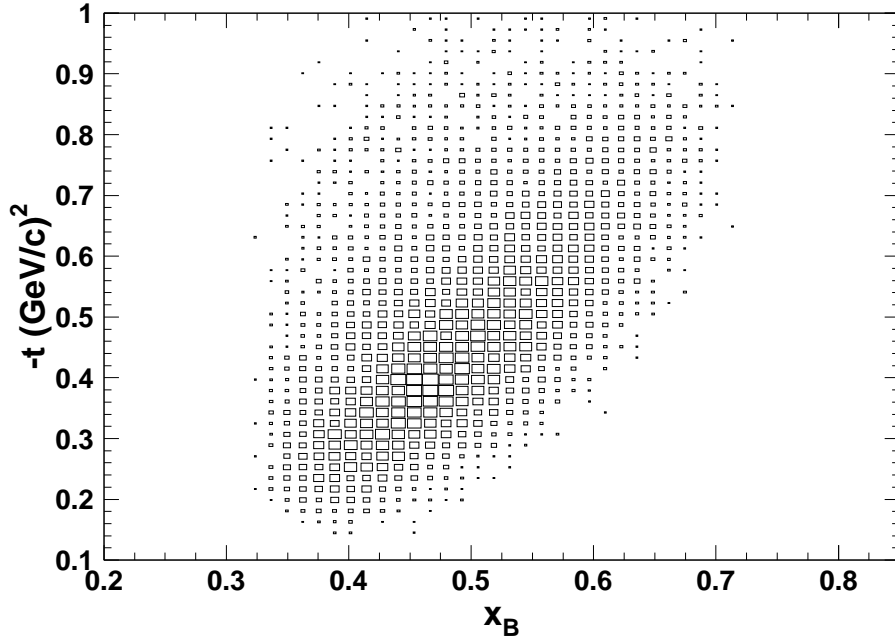


FIG. 8: Experimental acceptance in $-t$ and x_B for the $\epsilon = 0.32$ kinematic setting. In this case, cuts in Q^2 and x_B have already been implemented to match the low and high ϵ data, so the coverage is the same for the $\epsilon = 0.59$ setting.

less well studied, so for now we assume the longitudinal response is the same size as the transverse ($\sigma_L^y = \sigma_T^y$). We then used the Monte Carlo to simulate the relative $-t$ distribution of events for each ϵ setting, and determined the statistical uncertainty in fitting the constant ($\sigma_T + \epsilon\sigma_L$) and $\sin\beta$ ($\sigma_T^y + \epsilon\sigma_L^y$) terms of the unseparated cross sections.

As with any L-T separation, the uncertainty in the longitudinal piece is subject to the usual $1/\Delta\epsilon$ amplification. This means that we are the most sensitive to uncertainties that propagate randomly between ϵ settings. While there is a lot of experience in Hall C with L-T separations and their uncertainties, the calorimeter and target field make it more difficult to predict what these uncertainties will be. For the HMS-SOS set-up, it is typically assumed that uncorrelated errors in meson electroproduction experiments can be controlled to the 2–2.5% level. For now, we assume that the calorimeter + target field will increase these point-to-point errors and assume that the total uncorrelated portion of the uncertainty is on the order of 4%.

$-t$	$\langle x_B \rangle$	Counts	$\frac{\delta\sigma}{\sigma}_{stat} (\%)$	$\frac{\delta\sigma_L}{\sigma_L} (\%)$	$\frac{\delta\sigma^y}{\sigma^y}_{stat} (\%)$	$\frac{\delta\sigma^y_L}{\sigma^y_L} (\%)$
0.2–0.35	0.43	10650	1.0	20.8	4.7	31.2
0.35–0.5	0.48	14900	0.8	20.6	3.8	27.9
0.5–0.65	0.52	8940	1.1	20.9	4.8	31.5
0.65–0.8	0.55	3700	1.6	21.8	7.3	42.0

TABLE II: Projected statistical errors on the unseparated cross sections in each $-t$ -bin assuming a total of 40,000 events in the acceptance. Also shown is the total uncorrelated error on the longitudinal cross sections assuming 4% point-to-point systematic errors. The above calculations assume that the asymmetry (or longitudinal ratio) as defined in Eqn. 31 is 0.2, and that the (transverse) target polarization is 0.8. Note that if the asymmetry is significantly larger, the statistical precision on the σ^y_L improves for the same number of counts.

An example of the projected statistical and total uncorrelated error for each $-t$ -bin is shown in Table II. In the end, we need to take the ratio of cross sections to obtain the asymmetry, and in taking that ratio, some of the systematic errors that are typically uncorrelated when one determines an *absolute* separated cross section become partially correlated when one takes the ratio of separated cross sections. In the present estimates, we ignore these partially correlated errors, and treat all errors that are uncorrelated in the L-T separations as uncorrelated in the separated ratios as well.

Finally, the projected uncertainties for the transverse asymmetry are shown in Fig. 9. The uncertainties on these points ignore correlated uncertainties that should mostly cancel in the ratio. Note also that no uncertainty has been included for the target polarization. Assuming we can achieve 2-3% precision on this quantity, it is a minimal contribution to the uncertainty on the separated ratios. It is also worth mentioning that the unseparated ratio can be measured with very good precision (on the order of 5–10% relative) since the uncorrelated errors for σ^y_L and σ_L are still rather small when combined in quadrature at a particular ϵ .

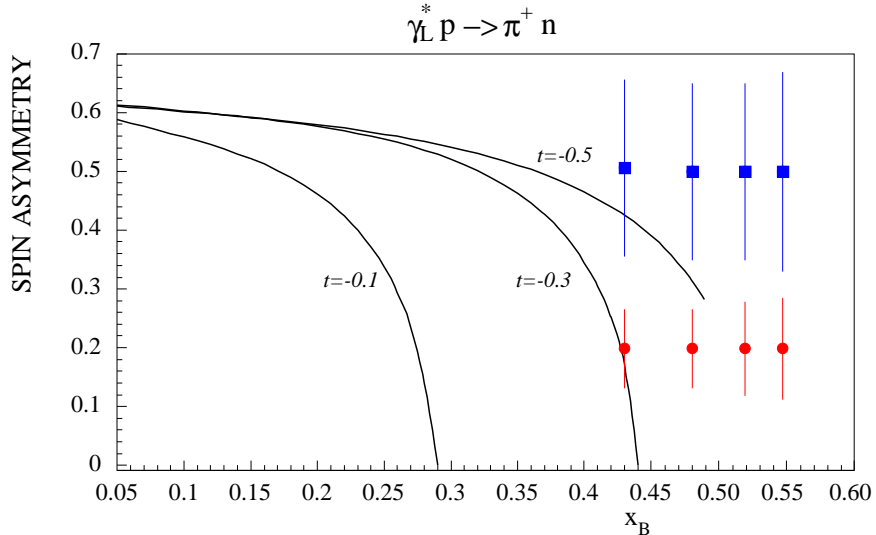


FIG. 9: Projected uncertainties for the L - T separated transverse target asymmetry, assuming $A_{\perp} = 0.2$ (red circles) and $A_{\perp} = 0.5$ (blue squares). Curves are predictions at various values of $-t$ from Ref. [10]. Each projected x_B point corresponds to the $-t$ range noted in Table II.

D. Further Studies

Before submitting a full proposal, there are of course several more studies that we would like to make. First, and perhaps the most significant, is that we need to examine the effect of target dilution on the asymmetry. Clearly, the unpolarized ^{15}N nuclei can also contribute to the measured π^+ yield, and this dilution will affect the measured asymmetry. Optimistically, one might think that due to kinematic correlations and the tight missing-mass constraint involved in measuring the $p(e, e'\pi^+)n$ reaction, this contribution from (largely) quasifree π^+ production from nuclei would be suppressed. However, this must be studied in more detail. We also would like to further study how well we can understand the acceptance of the combined BETA, HMS, and polarized target field set-up. Further considerations include the fact that we have assumed high precision beam current measurements at low currents. This is generally not a standard capability in Hall C and may require some new beamline components.

III. RELATION TO OTHER JLAB EXPERIMENTS

E-03-004: “Measurement of Single Target-Spin Asymmetry in Semi-Inclusive Pion Electroproduction on a Transversely Polarized ^3He Target”, was recently approved to run in Hall A. This experiment would measure the azimuthal distribution of π^- produced in the semi-inclusive $\vec{n}(e, e'\pi^-)X$ reaction, with the scattered electron detected in the Big-Bite spectrometer, and the π^- detected close to the virtual photon direction in the HRS_L. Although this experiment uses a transversely polarized target, the kinematics (semi-inclusive as opposed to exclusive pion production) and the motivation of this experiment (to differentiate between two competing mechanisms of neutron transversity) are completely different than ours.

LOI-03-002: “Transverse Polarization Effects in Hard Scattering at CLAS”. The dominant portion of this LOI deals with a proposed study of semi-inclusive pion electroproduction above the resonance region, to access distribution and fragmentation functions such as the transversity and the Collins and Sivers functions. Hard exclusive pion production is also mentioned as an important test of the applicability of GPD-based predictions at JLab energies.

While CLAS has a much larger acceptance than the BETA+HMS combination, our experiment will run at higher luminosity. A transversely polarized target for CLAS is only in the planning stages, but assuming the same thickness as the longitudinally polarized target used in E91-023, the existing UVa target is three times thicker. We will also be able to run at 85 nA as opposed to the typical 10 nA current used in CLAS. Finally, we will perform a precise Rosenbluth separation, minimizing questions about the interpretability of the result.

-
- [1] M. Diehl, arXiv:hep-ph/0010200.
 - [2] J.C. Collins, L. Frankfurt, M. Strikman, Phys. Rev. D **56** (1997) 2982.
 - [3] K. Goeke, M.V. Polyakov, M. Vanderhaeghen, Prog. Part. Nucl. Phys. **47** (2001) 401-515.
 - [4] A.V. Radyushkin, arXiv:hep-ph/0101225.
 - [5] A.W. Thomas, W. Weise, “The Structure of the Nucleon”, J. Wiley-VCH, 2001.

- [6] R.E. Marshak, Riazuddin, C.P. Ryan, “Theory of Weak Interactions in Particle Physics”, J. Wiley, 1969.
- [7] M. Penttinen, M.V. Polyakov, K. Goeke, Phys. Rev. C **62** (2000) 014024 1-11.
- [8] A.V. Belitsky, D. Mueller, Phys. Lett. **B 513** (2001) 349-360.
- [9] L.L. Frankfurt, P.V. Pobylitsa, M.V. Polyakov, M. Strikman, Phys. Rev. D **60** (1999) 014010 1-11.
- [10] L.L. Frankfurt, M.V. Polyakov, M. Strikman, M. Vanderhaeghen, Phys. Rev. Lett. **84** (2000) 2589-2592.
- [11] M. Vanderhaeghen, P.A.M. Guichon, M. Guidal, Phys. Rev. D **60** (1999) 094017 1-28.
- [12] A. Airapetian, et al., Phys. Lett. **B 535** (2002) 85-92.
- [13] L. Mankiewicz, G. Piller, A. Radyushkin, Eur. Phys. J. **C 10** (1999) 307-312.
- [14] C.E. Carlson, J. Milana, Phys. Rev. Lett. **65** (1990) 1717.
- [15] “The Science Driving the 12 GeV Upgrade of CEBAF”, February, 2001.
- [16] A. Bartl, W. Majerotto, Nucl. Phys. **B62** (1973) 267-285.
- [17] M. Vanderhaeghen, M. Guidal, J.-M. Laget, Phys. Rev. C **57** (1998) 1454.
- [18] J. Volmer, “The Pion Charge Form Factor via Pion Electroproduction on the Proton,” Ph.D. Thesis, Vrije Universiteit, 2000.
- [19] C. Harris, “The Proton Coulomb Form Factor from Polarized Inclusive $e-p$ Elastic Scattering at $Q^2 = 0.5$ (GeV/c) 2 ,” Ph.D. Thesis, University of Virginia, 2001.
- [20] D. Drechsel, O. Hanstein, S. S. Kamalov and L. Tiator, Nucl. Phys. A **645**, 145 (1999), <http://www.kph.uni-mainz.de/MAID/> (extended version).
- [21] It is interesting to note that a “conventional” asymmetry as it is typically defined is unnecessary. If one examines the β dependence of the difference of the cross section (or counts) between polarization states as defined in the lab, one will get zero since the very definition of β incorporates the direction of the target polarization.